



Identification of Potential Candidate Genes From Co-Expression Module Analysis During Preadipocyte Differentiation in Landrace Pig

Xitong Zhao^{1,2}, Huatao Liu², Yongjie Pan¹, Yibing Liu², Fengxia Zhang², Hong Ao³, Jibin Zhang⁴, Kai Xing^{5*} and Chuduan Wang^{2*}

¹Beijing Shunxin Agriculture Co., Ltd., Beijing, China, ²China Agricultural University, Beijing, China, ³Chinese Academy of Agricultural Sciences, Beijing, China, ⁴City of Hope National Medical Center, Duarte, CA, United States, ⁵Beijing University of Agriculture, Beijing, China

OPEN ACCESS

Edited by:

Linyang Xu,
Institute of Animal Sciences (CAAS),
China

Reviewed by:

Ligang Wang,
Institute of Animal Sciences (CAAS),
China

Yanghua He,
University of Hawaii at Manoa,
United States

*Correspondence:

Kai Xing
xk@bua.edu.cn
Chuduan Wang
cdwang@cau.edu.cn

Specialty section:

This article was submitted to
Livestock Genomics,
a section of the journal
Frontiers in Genetics

Received: 05 August 2021

Accepted: 08 December 2021

Published: 01 February 2022

Citation:

Zhao X, Liu H, Pan Y, Liu Y, Zhang F,
Ao H, Zhang J, Xing K and Wang C
(2022) Identification of Potential
Candidate Genes From Co-Expression
Module Analysis During Preadipocyte
Differentiation in Landrace Pig.
Front. Genet. 12:753725.
doi: 10.3389/fgene.2021.753725

Preadipocyte differentiation plays an important role in lipid deposition and affects fattening efficiency in pigs. In the present study, preadipocytes isolated from the subcutaneous adipose tissue of three Landrace piglets were induced into mature adipocytes *in vitro*. Gene clusters associated with fat deposition were investigated using RNA sequencing data at four time points during preadipocyte differentiation. Twenty-seven co-expression modules were subsequently constructed using weighted gene co-expression network analysis. Gene Ontology and Kyoto Encyclopedia of Genes and Genomes pathway enrichment analyses revealed three modules (blue, magenta, and brown) as being the most critical during preadipocyte differentiation. Based on these data and our previous differentially expressed gene analysis, angiopoietin-like 4 (*ANGPTL4*) was identified as a key regulator of preadipocyte differentiation and lipid metabolism. After inhibition of *ANGPTL4*, the expression of adipogenesis-related genes was reduced, except for that of lipoprotein lipase (*LPL*), which was negatively regulated by *ANGPTL4* during preadipocyte differentiation. Our findings provide a new perspective to understand the mechanism of fat deposition.

Keywords: pig, preadipocyte differentiation, lipid metabolism, WGCNA, siRNA

INTRODUCTION

The Landrace pig is a globally adopted lean-type breed owing to its fast growth rate and lower fat content (Poklucar et al., 2020). Fat deposition is an important trait in pigs as it significantly influences meat quality, fattening efficiency, reproductive performance, and immunity (Verbeke et al., 1999). Hyperplasia and hypertrophy of the adipocytes are the two main processes affecting fat deposition (Kershaw and Flier, 2004; Choe et al., 2016). Pluripotent mesenchymal stem cells develop into adipoblasts and further into preadipocytes. Subsequently, preadipocytes differentiate into adipocytes under specific conditions (Gregoire et al., 1998). Adipocyte stromal vascular (S-V) cells from young pigs contain more preadipocytes capable of attaching and differentiating into mature adipocytes than those from older pigs (Akanbi et al., 1994). According to previous research, 7 days is an appropriate time to isolate S-V cells (Zhou et al., 2007). Multiple key regulators in adipocyte differentiation have been identified. For example, tumor necrosis factor- α (TNF- α) inhibits adipocyte differentiation (Cawthorn and Sethi, 2008), whereas CCAAT/enhancer-

binding protein alpha (C/EBP α) regulates adipocyte terminal differentiation (Lane et al., 1999). Similarly, peroxisome proliferator-activated receptor gamma (PPAR γ) can induce adipocyte generation (Ricote et al., 1998), whereas sirtuin 1 (SIRT1) can negatively regulate PPAR γ to inhibit adipocyte differentiation (Picard et al., 2004). Adipose triglyceride lipase (Villena et al., 2004; Zimmermann et al., 2004), AMP-activated protein kinase (Yun and Zierath, 2006), SIRT1 (Cantó et al., 2010), perilipins (Greenberg et al., 1991; Londos et al., 1999), and hormone-sensitive lipase (Haemmerle et al., 2002) are involved in lipid metabolism.

Weighted gene co-expression network analysis (WGCNA) is a useful tool for exploring the complex relationships between genes and phenotypes in R (Langfelder and Horvath, 2008). WGCNA can transform gene expression data into a co-expression module that might be related to the phenotypic traits of interest (Horvath et al., 2006; Fuller et al., 2007; Shi et al., 2010; Udyavar et al., 2013). This method has been applied to various aspects of weighted correlation network analyses in studies on obesity (Morrison and Farmer, 2000; Kogelman et al., 2014; Kogelman et al., 2016). In pigs, WGCNA has been used to identify intramuscular fat-related gene sets (Zhao et al., 2020). Of note, gene interference has typically been used to determine gene function (Desaulniers et al., 2017; Chen et al., 2018).

Angiopoietin-like 4 (ANGPTL4), a secretory protein produced in the liver, kidneys, muscles, and adipose tissues (Singh et al., 2018), is a direct glucocorticoid receptor target that participates in glucocorticoid-regulated triglyceride (TG) metabolism (Koliwad et al., 2009). This protein is a strong regulator of lipid metabolism and obesity (Singh et al., 2018) and serves as an endogenous inhibitor of intestinal lipid digestion (Mattijssen et al., 2014). Although the regulatory role of ANGPTL4 in lipoprotein metabolism is well established, its contribution to the regulation of pig preadipocytes and lipid deposition is not fully understood. In the present study, we found that ANGPTL4 is associated with preadipocyte differentiation. We then determined its effect on preadipocyte differentiation using gene interference. Our study provides novel insights to understand the mechanism underlying fat deposition.

MATERIAL AND METHODS

Ethics Statement

All experimental procedures were performed following the Guide for Animal Care and Use of Laboratory Animals from the Institutional Animal Care and Use Committee at China Agricultural University. The experimental protocol was approved by the Department Animal Ethics Committee at China Agricultural University (Permit No. DK996).

Isolation of Preadipocytes and Induction of Their Differentiation

Three Landrace piglets from a pig breeding farm in Ninghe (Tianjin, China) were obtained for the present study. The piglets were euthanized at the age of 7 days through an

intraperitoneal injection of pentobarbital sodium (50 mg/kg body weight) and exsanguination. Subcutaneous adipose tissue samples were carefully resected under sterile conditions. The adipose tissue was digested with 0.1% type I collagenase (Sigma, Beijing, China) for approximately 2 h at 37°C and then centrifuged at 1,000 \times g for 8 min (Zhou et al., 2007). The resulting digestion mixture was successively filtered through 100- μ m mesh filters by centrifuging for 8–10 min to obtain preadipocyte pellets. The cell pellets were then resuspended in Dulbecco's modified Eagle's medium/nutrient mixture F-12 (DMEM/F12) containing 10% fetal bovine serum (FBS) and plated in glass culture dishes (Gibco, NY, United States). The culture medium was replaced every other day.

When the cells reached 90% confluence, they were transferred to six-well plates (Corning Costar, NY, United States) at a density of 3×10^6 cells/ml in 2 ml per well, incubated at 37°C with 5% CO₂ and 95% O₂, and cultured until 90% confluence. The standard culture medium was then replaced with adipogenic induction medium (DMEM containing 10% FBS, 0.5 mM 3-isobutyl-1-methylxanthine, 1 μ M dexamethasone, and 10 μ g/ml insulin; Sigma) and cultured for 2 days. The differentiation medium was then replaced with maintenance medium (DMEM containing 10% FBS and 10 μ g/ml insulin). Cell morphology was observed under a microscope. Twelve cell culture samples were obtained from each pig. The samples were collected from each pig at 0, 2, 4, and 8 days in triplicate and stored in liquid nitrogen until RNA isolation.

Identification of Lipid Droplets

Oil Red O staining was performed to identify lipid droplets. The cell culture plates were gently washed with phosphate-buffered saline (PBS) three times and fixed in 10% formaldehyde for 15 min. The cells were then washed with PBS three times and stained with Oil Red O for 20 min. Finally, the cells were washed three times with PBS and photographed using an inverted microscope (Leica, Wetzlar, Germany). An equal volume of 100% isopropanol solution was added to the wells of each culture plate, and the absorbance at 500 nm was measured after thoroughly homogenizing the samples. Each experiment was repeated three times.

RNA Isolation, Sequencing, and Sequence Data Processing

The total RNA was purified from the 12 samples using TRIzol reagent (Invitrogen, Carlsbad, CA, United States) according to the manufacturer's instructions. RNA quantity and quality were assessed using the Agilent 2100 Bioanalyzer (Agilent, Santa Clara, CA, United States). All RNA samples with RNA integrity numbers >8.0 and an absorbance 260:280 ratio >1.9 were selected for library construction and deep sequencing.

From each of the 12 samples, 10 μ g of RNA was used for RNA sequencing (RNA-seq) library preparation using the TruSeq® Stranded Total RNA Sample Preparation Kit (Illumina, CA, United States) according to the manufacturer's instructions. The ligation products were size-selected by agarose gel electrophoresis and amplified by PCR. After purification and

enrichment, 12 libraries were sequenced using the Illumina HiSeq 2500 system by Gene Denovo Biotechnology Co. (Guangzhou, Guangdong, China).

Raw reads were cleaned by removing adapter and primer sequences, reads containing more than 10% of unknown nucleotides (N), and more than 50% of low-quality (Q-value ≤ 20) bases. The clean reads were mapped to the pig reference genome (*Scrofa* 11.1, ftp://ftp.ensembl.org/pub/release-68/fasta/sus_scrofa/cdna) (Langmead et al., 2009) using Bowtie 2 (Langmead and Salzberg, 2012) and TopHat2 (version 2.0.3.12) (Trapnell et al., 2012) with default parameters. HT-seq (version 0.6.1) was used to calculate the read number mapped to each gene in each sample (Glaser et al., 2010).

Differential gene expression, based on the normalized read count of expressed genes, was analyzed in three time-point contrasts (0 vs. 2 days, 0 vs. 4 days, and 0 vs. 8 days) using the edgeR package (Robinson et al., 2009) in R (version 4.0.2). Genes with a false discovery rate (FDR) ≤ 0.05 and absolute \log_2 fold change ($|\log_2FC|$) > 1 were identified as differentially expressed genes (DEGs) between two groups (Zhao et al., 2019).

WGCNA

As mentioned previously, fat deposition is affected by preadipocyte differentiation. Thus, to identify candidate genes influencing preadipocyte differentiation, we applied WGCNA (Langfelder and Horvath, 2008) to fragments per kilobase of exon model per million mapped fragments (FPKM) values obtained from the RNA-seq of the 12 samples to identify genes associated with the degree of preadipocyte differentiation. Based on the expressed coding genes with FPKM > 0 , hierarchical clustering was performed. Outliers above a height threshold of 2,000 were filtered out. The remaining samples were used to establish an unsigned co-expression network.

We then used a one-step method to construct the network and determine the gene module. According to Zhang and Horvath (2005), gene co-expression networks should have scale-free characteristics and follow a power-law distribution. Hence, a weighted adjacency matrix was created, which can be defined as follows:

$$A_{ij} = |cor \times (x_i, x_j)|^\beta, \quad (1)$$

where x_i and x_j are the i th and j th genes, respectively.

Adjacent to the adjacent network is the combination of the soft-thresholding power parameter β , which is required to improve the co-expression similarity for computing the adjacency. To keep the network consistent with scale-free topology, the pickSoftThreshold() function in R was used to analyze its topology and select an appropriate soft-thresholding power value (β) to build it, and the mean connectivity of all genes in the module was evaluated. A power of 18 was selected as the soft threshold to ensure a scale-free topology network ($R^2 = 0.85$).

Subsequently, the topology overlap matrix (TOM) (Zhang and Horvath, 2005), which measures the connectivity of a pair of genes, was calculated from the adjacency matrix. Once the power

value was determined, the TOM and $dissTOM = 1 - TOM$ were obtained. Based on hierarchical average linkage clustering using a dynamic tree-cutting algorithm, genes with similar expression patterns were clustered into the same modules and assigned a color (Zhang and Horvath, 2005).

After construction, the module eigengene (ME) was calculated using the first principal component of the expression profiles, which represented the weighted average expression profile. To identify biologically significant modules and select potentially critical modules for downstream analysis, the WGCNA approach was used to define the module-trait relationships (MTRs) (Kogelman et al., 2014) and gene significance (GS) of each module (Liu et al., 2016). We considered the time point of cell differentiation as a dichotomous variable (Langfelder and Horvath, 2008). A Pearson's correlation test was run between the ME and time point of cell differentiation and between the expression profiles and time point of cell differentiation to estimate the MTRs and GS, respectively. The module significance (MS) was the mean GS value of the module genes. According to the selection criteria for critical modules reported in a previous study, modules with $MTR > 0.30$ and $MS > 0.25$ were considered candidate modules for functional enrichment analysis (Howard et al., 2017). Highly connected genes, also known as hub genes, may play important roles in a module (Wilhelm et al., 2004). Hub genes are relatively conserved at the core of the gene co-expression network, which can act as a genetic buffer to reduce the effect of other gene mutations (Kadioglu et al., 2021). Here, genes with $GS > 0.3$, module membership (MM) > 0.85 , and intramodular connectivity > 5 were considered hub genes. Cytoscape (Shannon et al., 2003) was used to map the gene-gene interaction network for visualizing gene relationships.

Functional Enrichment Analysis of Co-expression Modules and Selection of Candidate Genes

Gene Ontology (GO; <http://www.geneontology.org/>) is widely used in the field of bioinformatics to classify genes into terms from three different biological categories: cellular components, molecular functions, and biological processes. The default values were adapted for the parameters of the phenotype-related module, and three GO term enrichment analyses were performed on the genes in the module. Adjusted p -values < 0.05 were considered significant, and the 10 most prominent entries for each analysis were retained.

Kyoto Encyclopedia of Genes and Genomes (KEGG, <http://www.genome.jp/kegg/>) is a database for systematic analysis of gene function and genomic information that facilitates the study of genes and gene expression as a part of an entire network. "ClusterProfiler" (Yu et al., 2012) and "ggplot2" packages were used to analyze and visualize such genetic information, respectively. The R package BioMart (<http://www.biomart.org/>) (Haider et al., 2009) was used to annotate genes in the module with *Sscrofa11.1* as a reference genome. We selected a subset of modules based on their functional annotation and selected genes related to fat development. Based on the above information, the candidate

TABLE 1 | siRNA sequences designed for *ANGPTL4*.

Plasmid name	siRNA sequences
si-752	5'-GGGACUGCCAGGAACUCUUTT-3' 5'-AAGAGUUCUGGCAGUCCCTT-3'
si-398	5'-GCAUGGCUGCCUGUGUAATT-3' 5'-UUACCACAGCCAGCCAUGCTT-3'
si-1376	5'-CCCUGCUGAUCCAGCCCAUTT-3' 5'-AUGGGCUGGAUCAGCAGGGTT-3'
Negative control	5'-UUCUCCGAACGUGUCACGUTT-3' 5'-ACGUGACACGUUCGGAGAATT-3'

genes affecting fat deposition were determined in this experiment.

ANGPTL4 Knockdown

In our previous study (Zhao et al., 2019), *ANGPTL4* was identified as a DEG in all time-point contrast groups and was related to the PPAR signaling pathway and cell differentiation process. Similarly, in the present study, *ANGPTL4* was identified in a key module; therefore, we hypothesized that *ANGPTL4* has some regulatory effects on preadipocyte differentiation. According to the sequence of pig *ANGPTL4* (ID: 397,628) in GenBank, three pairs of siRNAs targeting and corresponding negative controls were designed and synthesized by GenePharma (Suzhou, Jiangsu, China) (Table 1). The siRNAs were centrifuged at 10,000 rpm for 2 min and dissolved in 125 μ l of Nuclease-Free Tubes, Tips, and Buffers (DEPC) water (Gibco, NY, United States) to a final concentration of 20 μ mol/L.

Once the cell confluence reached 70%–80%, Lipofectamine 2000 (Invitrogen) was used for transfection. According to the manufacturer's instructions, the medium was replaced with 2.5 ml of DMEM/F12 medium without serum and antibody, 30 min before transfection. Thereafter, 5 μ l of Lipofectamine 2000 was diluted with 250 μ l of serum and double-antibody-free DMEM/F12 medium per well, mixed gently, and incubated at room temperature (21°C–25°C) for 5 min; this was mixture I. Next, 10 μ l of siRNA was collected from each well, diluted with 250 μ l of serum-free and double-resistant DMEM/F12 medium, mixed gently, and incubated at RT for 5 min; this was mixture II. Mixtures I and II were gently mixed and allowed to stand for 20 min at RT. Thereafter, mixtures I and II were added to each well to a total volume of 500 μ l and mixed thoroughly. After incubation at 37°C for 6 h, the medium was replaced with a complete medium. These steps were followed to induce cells and were repeated three times for each experiment.

RNA Extraction and Quantitative Reverse-Transcription Quantitative Polymerase Chain Reaction

Based on our previous study (Zhao et al., 2019), *ANGPTL4* has the same expression pattern as Acetyl CoA acyltransferase 2 (*ACAA2*), aldehyde dehydrogenase two family member (*ALDH2*), and solute carrier family 27 member 1 (*SLC27A1*). Furthermore, lipoprotein lipase (*LPL*), stearoyl-CoA desaturase (*SCD*), and fatty acid synthase (*FASN*) are markers of fat

deposition. Thus, we observed whether the expression of those genes changed before and after the interference of *ANGPTL4*.

The total RNA was extracted using a TRIzol reagent (Invitrogen) and reverse-transcribed into cDNA according to the manufacturer's instructions. Reverse-transcription quantitative polymerase chain reaction (RT-qPCR) was performed using the Light Cycler 480 Real-Time PCR system (Roche, Hercules, CA, United States). The primers used for RT-qPCR detection of the selected genes are listed in **Supplementary Table S1**. All RT-qPCR experiments were performed using three biological replicates with three technical replicates for each sample. The $2^{-\Delta\Delta Ct}$ method was used to measure the change in mRNA abundance, and glyceraldehyde 3-phosphate dehydrogenase (*GAPDH*) was used as the internal control.

Statistical Analyses

All qRT-PCR results are presented as mean \pm standard deviation (SD). Statistical analyses were conducted using SPSS software (version 20.0; IBM Corp., Armonk, NY, United States); results with $p < 0.01$ were considered extremely significant, and those with $p < 0.05$ were considered significant.

RESULTS

Phenotypic Changes During Preadipocyte Differentiation

Compared to cell shapes observed during the initial phase (day 0), preadipocytes gradually changed from fibrous to spherical on day 2. Subsequently, lipid droplets became visible on day 4, gradually increasing in number until day 8 (Figure 1). These results indicated that the preadipocytes differentiated successfully and could be used for further analysis.

Construction of Co-expression Modules

Genes with a sum of FPKM values >0 ($n = 12,816$) were selected for a co-expression network analysis (Supplementary Table S2). The WGCNA package in R was used to construct co-expression modules. No outlier samples were found in the hierarchical clustering of samples using the flashClust package in R (Supplementary Figure S1).

According to the standard of a scale-free network, we selected an appropriate weighted parameter of the adjacency function, namely, the soft threshold, which was 18 in this study (Supplementary Figure S2). We then calculated the correlation and adjacency matrices and combined them into the topology matrix. We finally identified 27 gene modules based on genetic similarity after merging modules with dissimilarities less than 0.25 and a minimum size of 30 (Figure 2; Supplementary Table S3).

Analysis of the Relationship Between Gene Modules and Preadipocyte Differentiation

The Pearson correlation coefficient between the eigengenes of modules and the corresponding variables represents the linear correlation between the module and phenotypic information

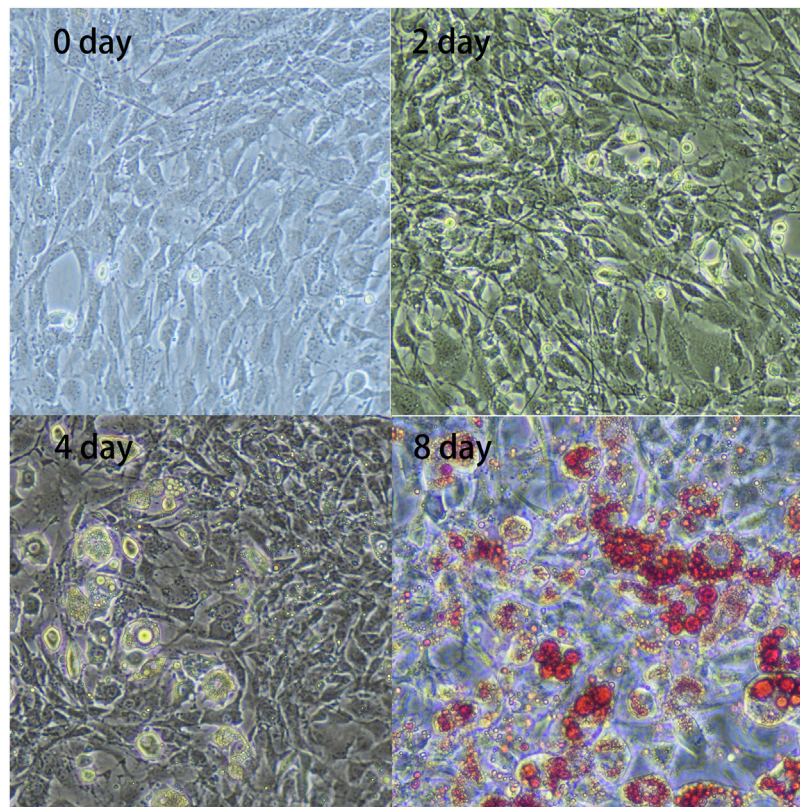


FIGURE 1 | *In vitro* adipocyte differentiation. Preadipocytes were obtained from the subcutaneous adipose tissue of three 7-day-old Landrace pigs and were cultured and collected at four differentiation stages: 0, 2, 4, and 8 days. The figure shows enlarged representative photographs of adipocytes obtained during differentiation [day 0, 2, 4, and 8; day 8 with Oil Red O staining (x20)].

(**Figure 3**). We found that the blue and brown modules were significantly correlated with day 8 ($r = 0.59$, $p < 0.05$; **Figure 3**), which was the time point with the most preadipocytes, suggesting that genes in these two modules promote preadipocyte differentiation. In addition, the magenta module was significantly correlated with day 0 when there was little differentiation ($r = 0.78$, $p < 0.01$), suggesting that these genes inhibit preadipocyte differentiation.

As a final module assessment, scatter plots of GS for preadipocyte differentiation versus MM for the blue, brown, and magenta modules are presented in **Figure 4**. We found a significant correlation between GS and MM, suggesting that genes in the preadipocyte differentiation-related modules tended to highly correlate with fat deposition.

Functional Enrichment Analysis of Genes in Candidate Modules

For the genes in the blue, brown, and magenta modules, GO term and KEGG pathway enrichment analyses were performed (**Table 2**, **Table 3**). We found that genes in the blue module play a role in fatty acid degradation, those in the brown module play a role in mitogen-activated protein kinase (MAPK) signaling pathways, and genes in both modules participate in fatty acid

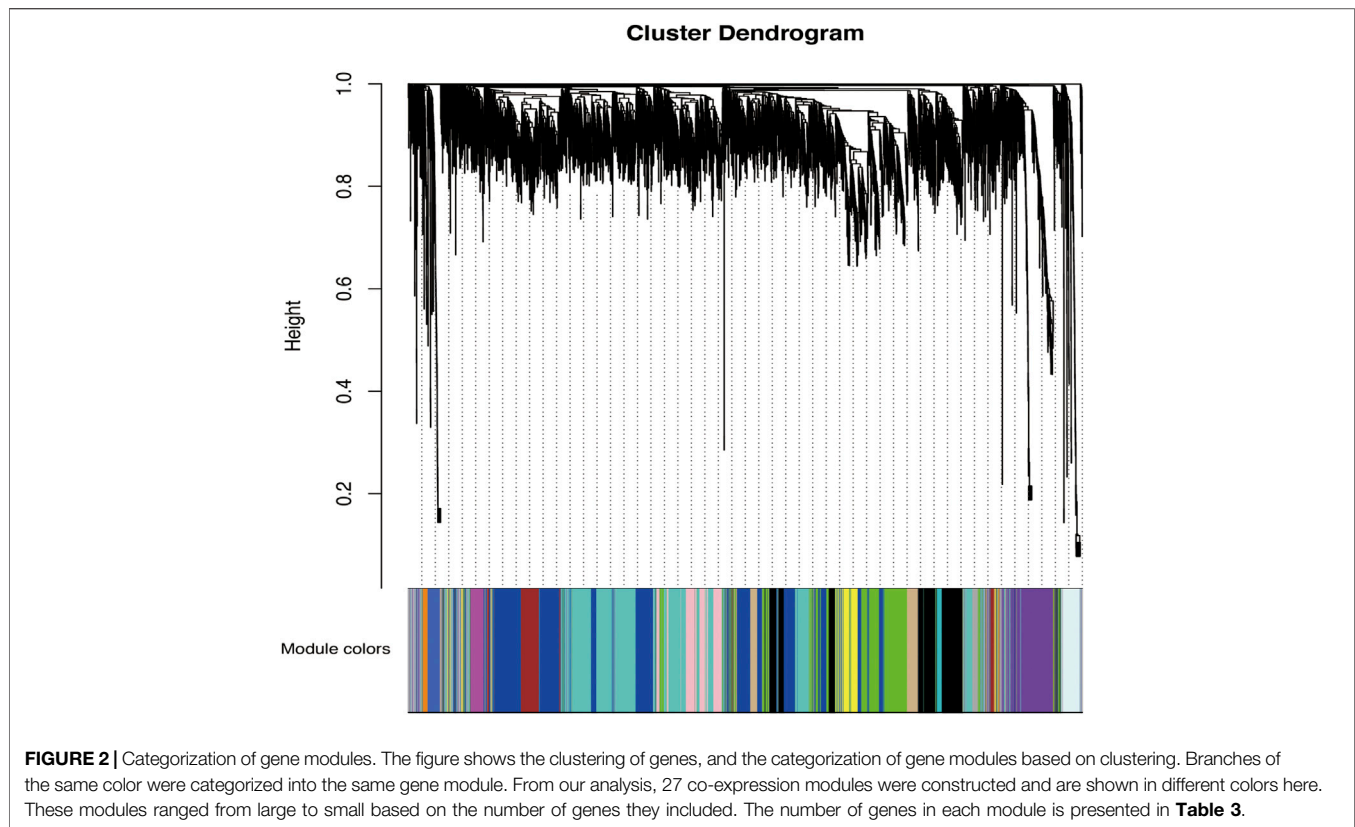
beta-oxidation. Genes in the magenta module are related to fatty acid beta-oxidation using acyl-CoA dehydrogenase, the Wnt/PI3K-Akt/TGF-beta signaling pathway, and the regulation of stem cell pluripotency. These results suggested that genes in the blue, brown, and magenta modules are related to lipid metabolism.

Module Visualization and Hub Genes

Genes with the highest degree of connectivity were selected from the three candidate modules, and Cytoscape software was used to draw the gene interaction network diagrams (**Figure 5**). We found *ANGPTL4* in the blue module (**Supplementary Table S4**). Thus, we knocked down *ANGPTL4* to observe its effect on preadipocyte differentiation.

Transfection Efficiency of siRNAs and Analysis of the mRNA Expression of the Related Genes

Three pairs of siRNAs were synthesized. The expression level of *ANGPTL4* was determined 0, 2, 4, and 8 days after differentiation following transfection (**Figure 6**). The transfection efficiency of siRNA-752 was the highest (>90%); thus, it was used in the subsequent experiments.



As shown in **Figure 7A**, the mRNA levels of *ANGPTL4*, *ACAA2*, *SLC27A1*, *ALDH2*, *PPAR*, *SCD*, *FASN*, and *LPL* increased with preadipocyte differentiation. After transfection, we observed changes in the expression levels of these genes. The expression level of *ANGPTL4* significantly decreased, confirming successful transfection. Except for *LPL*, whose expression level was opposite to that of *ANGPTL4*, the expression of the other genes initially increased and then decreased (**Figure 7B**).

Effects of *ANGPTL4* Knockdown on the Differentiation of Pig Preadipocytes

Two days after transfecting preadipocytes with siRNA-752, the inducer was added to promote differentiation. The cells were then stained with Oil Red O and observed under a microscope. Compared with the negative control group, the siRNA-752 transfection group showed a significant increase in lipid droplet production (**Figures 8A,B**) and OD_{500nm} values ($p < 0.05$) (**Figure 8C**), indicating that the knockdown of *ANGPTL4* promoted the differentiation of porcine preadipocytes.

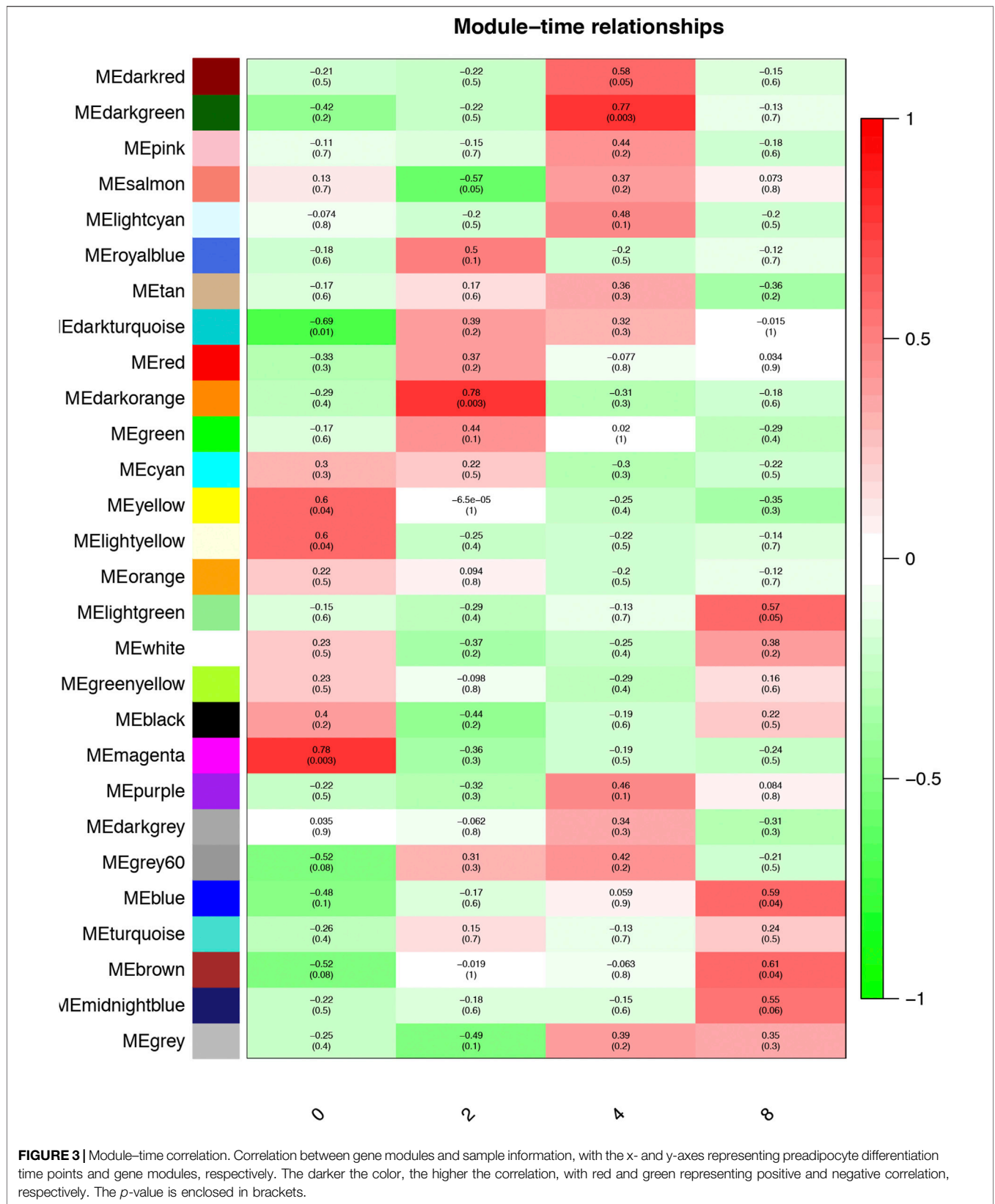
DISCUSSION

Lipid metabolism is a pivotal factor in maintaining health and determining fat deposition (Mourot and Hermier, 2001). However, given the complex and dynamic nature of lipid metabolism regulation (Kahn and Flier, 2000), we do not yet

fully understand the role of genes in this process. In the present study, we performed WGCNA using the RNA-seq data of Landrace preadipocytes to identify fat deposition-related genes.

We constructed 27 co-expression modules with 12,816 genes from 12 pig preadipocyte samples collected at four time points using the WGCNA method to identify genes involved in preadipocyte differentiation. WGCNA offers several distinct advantages over other methods; for instance, it allows an analysis to focus directly on the association between co-expression modules and lipid metabolism (Shubham et al., 2017; Hu et al., 2018; Li et al., 2018). Genes in the same module are generally connected to the same terms of function. Therefore, the analysis enabled the identification of biologically relevant modules and hub genes that may eventually serve as biomarkers for diagnosis or treatment.

Three modules were the most closely related to preadipocyte differentiation. The blue and brown modules were significantly correlated with day 8 and may be related to lipid deposition. Conversely, the magenta module was significantly correlated with day 0 and may play an inhibiting role in adipocyte differentiation. The GO term and KEGG pathway enrichment analyses showed that the blue module was related to fatty acid beta-oxidation, fatty-acyl-CoA binding, and fatty acid degradation. The brown module was related to fatty acid beta-oxidation and MAPK signaling pathways, which are activated in response to a variety of extracellular stimuli, such as growth factor stimulation, and play an important role in lipid localization (Anderson, 2006).



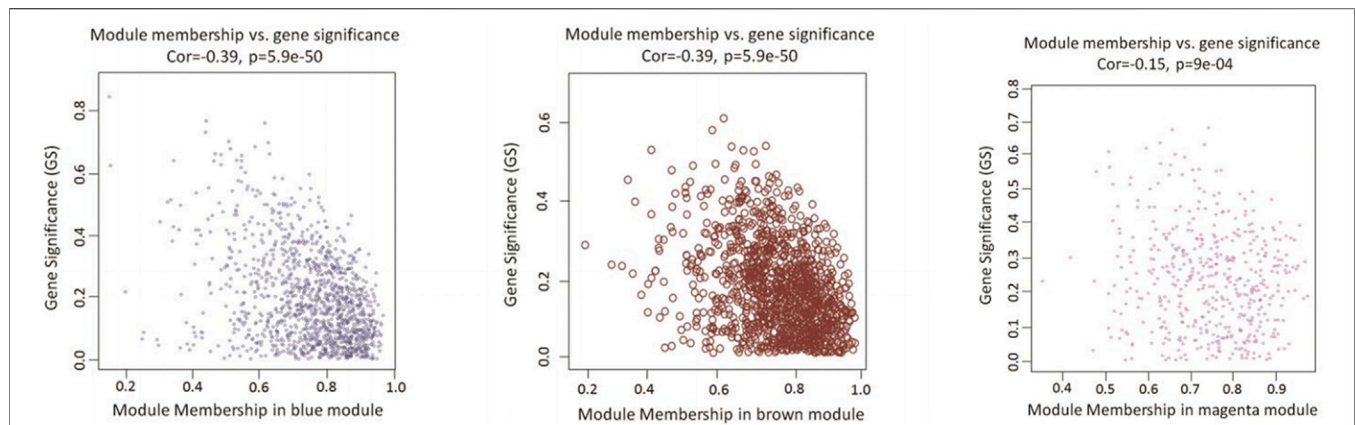


FIGURE 4 | Scatterplots of GS vs. MM in candidate modules. The figure shows the GS in the three significant modules correlated with adipocyte differentiation. The x-axis represents the value of membership in each module, and the y-axis represents the GS of the genes in the blue, brown, and magenta modules. The gene in the lower right corner of each graph is the hub gene that is of interest to us. These genes are highly correlated with phenotypes and have a high MM, which is a good representation of the gene module.

TABLE 2 | GO terms of candidate modules (adjusted *p*-value ≤ 0.05).

Module	Term ID	Term name	<i>p</i> -value	Genes
Blue	GO:0006635	Fatty acid beta-oxidation	2.04E-02	EC11, ACAA2, PEX5, ABCD3, BDH2, ACAT1, ACAA1, ANGPTL4
	GO:0000062	Fatty-acyl-CoA binding	2.78E-02	GCDH, ECI2, ACADSB, ACADS, ACBD6, ACBD4
Brown	GO:0006635	Fatty acid beta-oxidation	1.67E-02	ECHDC2, HIBCH, HSD17B4, SESN2, CROT, ACOX3, AUH
Magenta	GO:0033539	Fatty acid beta-oxidation using acyl-CoA dehydrogenase	1.11E-02	ACADVL, ETFDH, ACAD9, ETFB
	GO:0090263	Positive regulation of canonical Wnt signaling pathway	2.37E-02	DKK2, CAV1, SFRP2, COL1A1, LRRK1, SRC

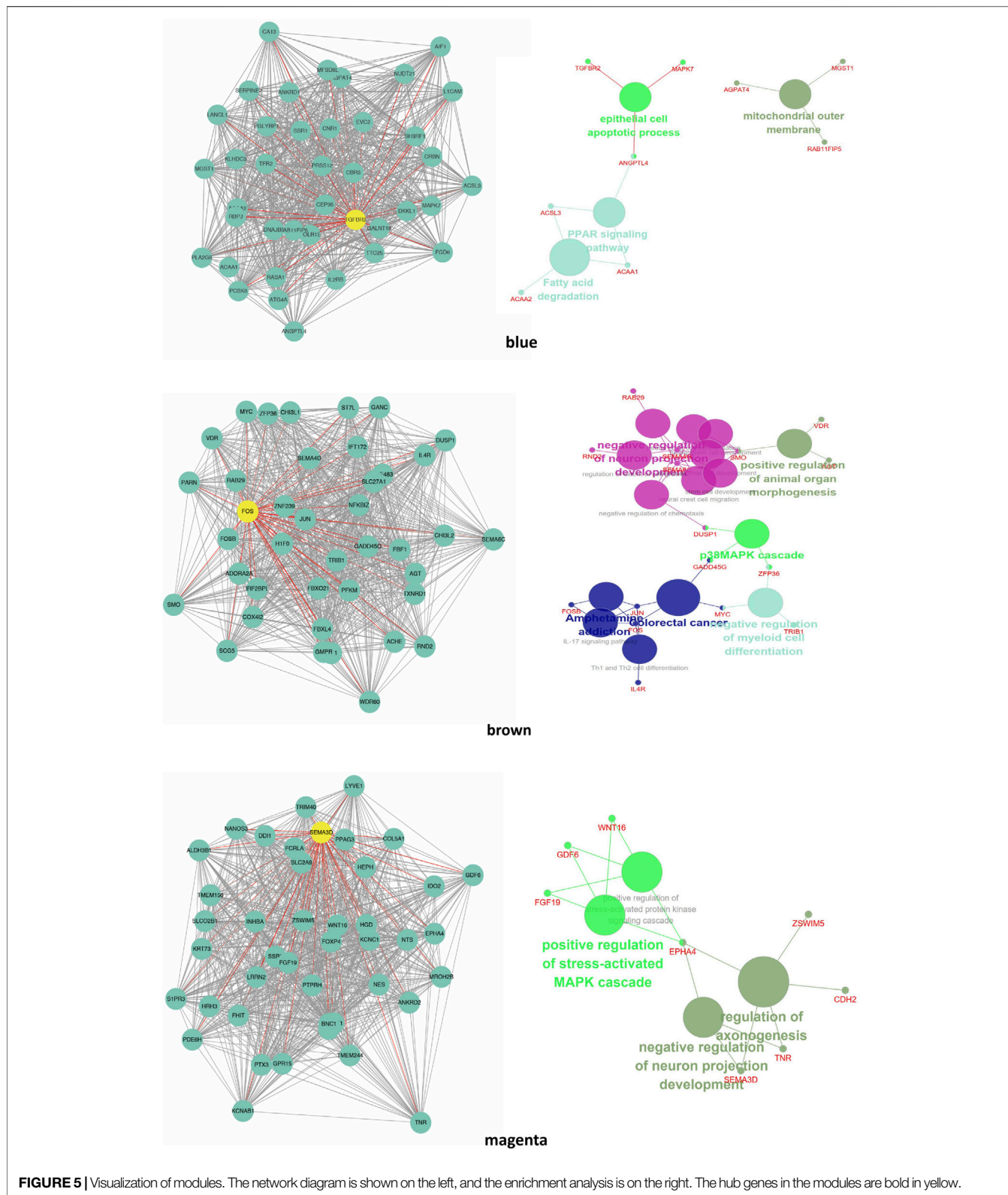
TABLE 3 | KEGG analysis of candidate modules (adjusted *p*-value ≤ 0.05).

Modules	Term	<i>p</i> -value	Genes
Blue	cfa00071:Fatty acid degradation	2.05E-04	EC11, GCDH, ECI2, ACAA2, ACADSB, ALDH7A1, ACADS, ACAT1, ACSL3, ALDH9A1, ACSL5, ACAA1
Brown	ptr04010:MAPK signaling pathway	5.15E-03	FGFR1, IL1R1, FGFR4, MAP4K2, CACNB1, MAPKAPK3, MKNK1, FOS, JUND, MAP3K8, PPP3CC, PRKACB, MYC, TAOK2, CACNG7, CACNG5, MAPK10, TAB1, DUSP5, NRAS, DUSP1, JUN, NTRK1, GADD45G, GADD45B, MAP3K12, DUSP7, DUSP6
Magenta	cfa04151:PI3K-Akt signaling pathway	2.76E-02	FGF19, IBSP, FGF18, FGF5, IL7, PDGFA, COL3A1, COL5A2, COL5A1, SOS1, TNFR, COL6A2, COL1A2, LAMC1, COL1A1, PIK3R3, LAMB1
	cfa04350:TGF-beta signaling pathway	2.61E-02	INHBA, GDF6, CREBBP, BMPR2, TGFB3, BMPR1B, ACVR1
	cfa04550:Signaling pathways regulating pluripotency of stem cells	5.11E-03	WNT10A, INHBA, WNT16, BMPR2, WNT9A, PIK3R3, BMPR1B, WNT6, MEIS1, TCF3, ACVR1

The magenta module was found to be involved in the positive regulation of the canonical Wnt signaling pathway. Wnt/ β -catenin signaling is the central negative regulator of adipogenesis (Ross et al., 2000; Bennett et al., 2002) and is related to lipid accumulation (Tian et al., 2019). Additionally, the magenta module was enriched in signaling pathways regulating the pluripotency of stem cells, which might be related to preadipocyte proliferation. These findings suggest that the expression of genes in the blue and brown modules

increased with hypertrophy, whereas the genes in the magenta module contributed to hyperplasia.

We then identified hub genes in the three co-expression modules. The hub gene in the magenta module was semaphorin 3D (*SEMA3D*), which promotes cell proliferation (Berndt, 2006) and may be involved in regulating cell sorting (Lallier, 2004). The hub gene in the brown module was the Fos proto-oncogene AP-1 transcription factor subunit (*FOS*), which belongs to the JUN family and is a regulator of cell proliferation,



differentiation, and transformation (Karin et al., 1997; Shaulian and Karin, 2001). *FOS* may also be related to lipid homeostasis (Izawa et al., 2015). These hub genes are potential biomarkers for

preadipocyte differentiation and lipid metabolism and require further research. The hub gene of the blue module was transforming growth factor-beta receptor 2 (*TGFBR2*), which

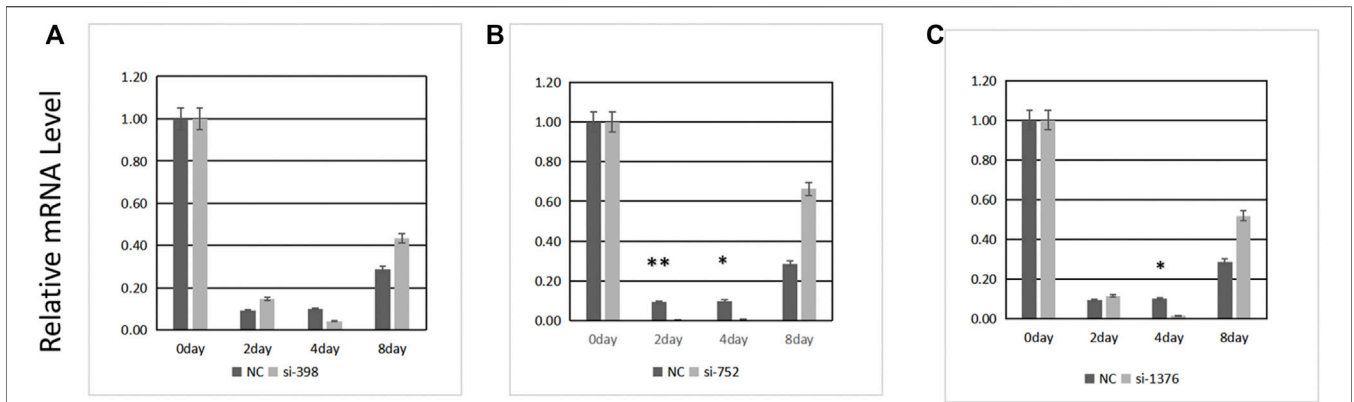


FIGURE 6 | Transfection efficiency of three siRNAs. **(A)** si-398, **(B)** si-752, **(C)** si-1376. *Significant ($p < 0.05$), **extremely significant ($p < 0.01$).

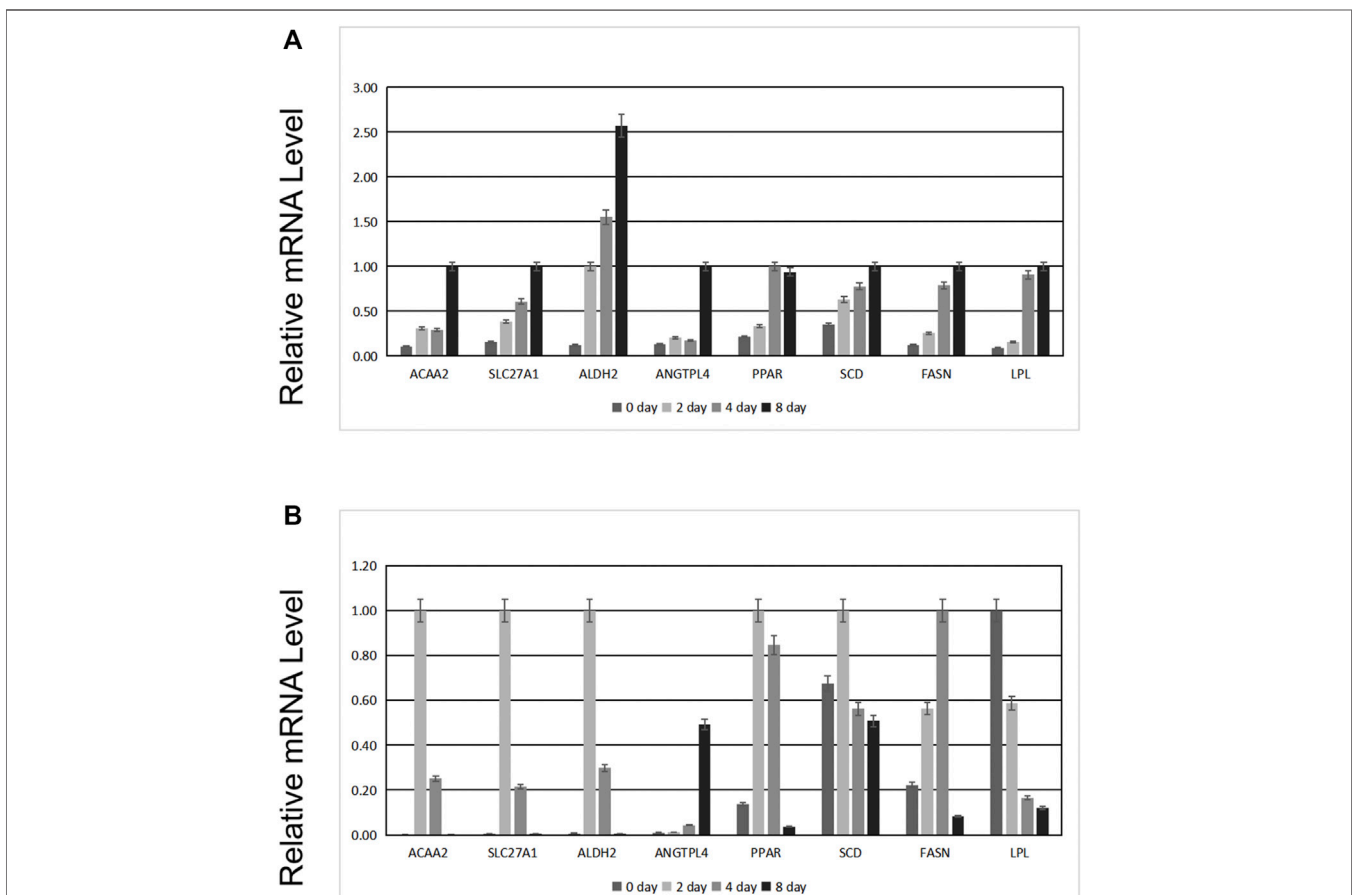
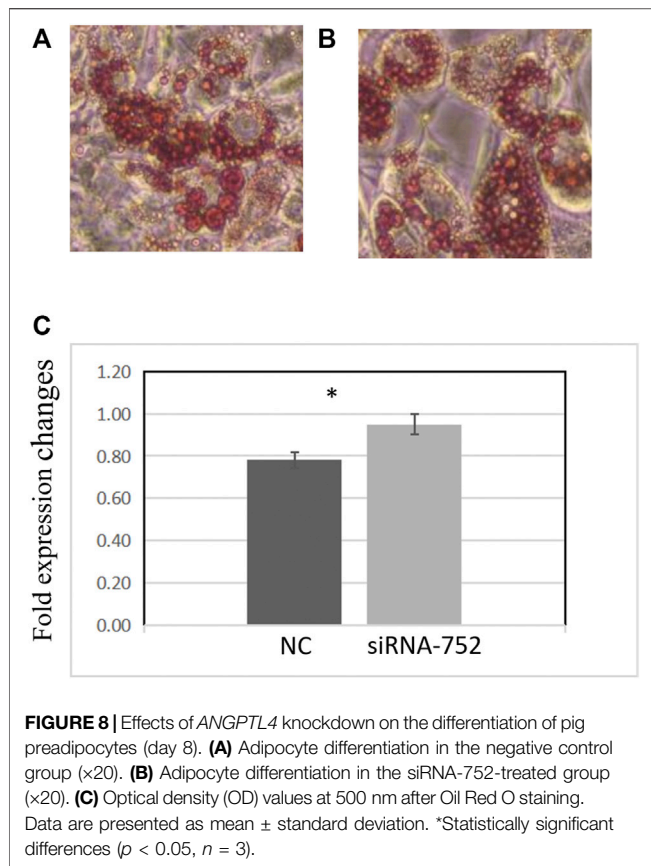


FIGURE 7 | Effects of *ANGPTL4* knockdown on the mRNA expression levels of the related genes. **(A)** Expression before transfection of siRNA. **(B)** Expression after transfection of siRNA.

is related to cell apoptosis and cell cycle arrest (Oft et al., 1998). *TGFBR2* may influence lipid metabolic activities through TGF- β signaling (Iwata et al., 2014). In addition, *ANGPTL4* and *ACAA2* in the blue module were found in the same cluster as that in our previous study (Zhao et al., 2019). *ACAA2* is a key enzyme in the

fatty acid oxidation pathway that catalyzes the last step of mitochondrial beta-oxidation, thus playing an important role in fatty acid metabolism (Sodhi et al., 2014; Wang et al., 2016). Beta-oxidation of fatty acids may affect muscle fat content by changing the content of fatty acids, which may ultimately affect



meat quality. Similarly, a previous study reported that *ACAA2* promotes sheep preadipocyte differentiation (Zhang et al., 2019) and is related to swine fat deposition (Xing et al., 2015). *ANGPTL4*, which is in the same module as *ACAA2*, may have similar functions.

In this study, we inhibited *ANGPTL4* expression and observed the changes in the mRNA levels of related genes. We found that although fewer fat droplets were produced, the process of adipocyte differentiation was still completed, suggesting that lipid metabolism is a complex process influenced by multiple factors and is not offset by a single gene. However, it is important to note that we interfered with gene expression with an approximate efficiency of 90% and did not completely knock out *ANGPTL4*. Therefore, it is possible that trace amounts of the target gene product continued to play a role. This is a limitation of this study that needs to be addressed in future studies.

After the inhibition of *ANGPTL4* expression, only the expression trend of *LPL* was different from that of other genes. This may confirm the suggestion of several studies that *ANGPTL4* negatively regulates *LPL*. Plasma TG levels are primarily determined by the dynamic balance between TG absorption in the small intestine and TG degradation in muscles and adipose tissues (Rosen and MacDougald, 2006). *LPL* is particularly important as a rate-limiting enzyme for the hydrolysis of TGs in the blood (Yagyu et al., 2003). This enzyme is produced by muscle cells and

adipocytes, transported to the surface of endothelial cells after binding with glycosylphosphatidylinositol-anchored high-density lipoprotein binding protein 1 (GPIHBP1) (Davies et al., 2010), and primarily regulated at the post-translational level (Ogata and Oku, 2001). *ANGPTL4*, as an equilibrium switch that regulates homeostasis, increases blood TG levels by inhibiting *LPL* activity (Yoshida et al., 2002). *ANGPTL3* and *ANGPTL8*, which are members of the same angiopoietin-like protein family as *ANGPTL4*, might also participate in the regulation of *LPL*, and their coordination ensures the balance of TG levels. *ANGPTL3* and *ANGPTL4* are inhibitors of *LPL* activity, and *ANGPTL8* inhibits *LPL* secretion (Kovrov et al., 2019). During exercise, fasting, and cold exposure, *ANGPTL4* inhibits *LPL* activity in the adipose tissues, skeletal muscles, and heart; inhibits *LPL*-mediated circulating TG clearance; reduces the entry of plasma TG-derived fatty acids into adipose tissues; and promotes their absorption by oxidized tissues (Kroupa et al., 2012; Catoire et al., 2014; Dijk et al., 2015). However, the inhibition of *LPL* by *ANGPTL4* is rapidly eliminated after the stable binding of GPIHBP1 with the dimer form of *LPL* (Sonnenburg et al., 2009). Fasting reportedly induces higher expression of *ANGPTL4* in the adipose tissues, and it reduces *LPL* activity by promoting protease lysis of *LPL* in cells (Dijk et al., 2018). *ANGPTL4* derived from mouse brown adipose tissue also inhibits *LPL* activity and promotes thermogenesis (Singh et al., 2018). The knockout of *ANGPTL4* in mice increases body fat and weight (Mattijssen et al., 2014). Some scientists believe that *ANGPTL4* and *LPL* are involved in a specific pathway. For instance, a previous study found that the overexpression of *miR-134* reduces the expression of *ANGPTL4* in the aortic tissues and peritoneal macrophages, while increasing the expression and activity of *LPL* and promoting lipid accumulation and pro-inflammatory cytokine secretion, thus accelerating the formation of atherosclerotic plaques (Ye et al., 2018). Our results are consistent with those of previous reports, suggesting that *ANGPTL4* and *LPL* form a pathway in pigs, where *ANGPTL4* negatively regulates *LPL*. However, further studies are required to validate our findings.

CONCLUSION

In this study, 27 co-expression modules were constructed using 12,816 genes from 12 pig preadipocyte samples via the WGCNA method. Three modules were identified as being the most critical during preadipocyte differentiation. Through WGCNA and DEG analysis, the hub gene *ANGPTL4* was identified as a potential regulator of preadipocyte differentiation and lipid metabolism. Following *ANGPTL4* inhibition, the expression of adipogenesis-related genes was also reduced, except for *LPL*. *ANGPTL4* could negatively regulate *LPL* during preadipocyte differentiation. Our findings provide a new perspective for understanding the mechanism underlying fat deposition.

DATA AVAILABILITY STATEMENT

The datasets presented in this study can be found in online repositories. The names of the repository/repositories and accession number(s) can be found below: NCBI (accession: PRJNA509755).

ETHICS STATEMENT

This animal study was reviewed and approved by the Departmental Animal Ethics Committee of China Agricultural University (Permit No. DK996).

AUTHOR CONTRIBUTIONS

Conceptualization, HA, CW, and KX; methodology, XZ and FZ; software, XZ and KX; validation, XZ and HL; formal analysis, XZ; investigation, XZ; data curation, XZ; writing—original draft preparation, KX; writing—review and editing, XZ, KX, JZ, and YL; supervision, CW and KX; project administration, HA and YP; funding acquisition, CW.

REFERENCES

- Akanbi, K. A., Brodie, A. E., Suryawan, A., and Hu, C. Y. (1994). Effect of Age on the Differentiation of Porcine Adipose Stromal-Vascular Cells in Culture. *J. Anim. Sci.* 72, 2828–2835. doi:10.2527/1994.72112828x
- Anderson, D. H. (2006). Role of Lipids in the MAPK Signaling Pathway. *Prog. Lipid Res.* 45, 102–119. doi:10.1016/j.plipres.2005.12.003
- Bennett, C. N., Ross, S. E., Longo, K. A., Bajnok, L., Hemati, N., Johnson, K. W., et al. (2002). Regulation of Wnt Signaling during Adipogenesis. *J. Biol. Chem.* 277, 30998–31004. doi:10.1074/jbc.M204527200
- Berndt, J. D., and Halloran, M. C. (2006). Semaphorin 3d Promotes Cell Proliferation and Neural Crest Cell Development Downstream of TCF in the Zebrafish Hindbrain. *Development* 133, 3983–3992. doi:10.1242/dev.02583
- Cantó, C., Jiang, L. Q., Deshmukh, A. S., Matak, C., Coste, A., Lagouge, M., et al. (2010). Interdependence of AMPK and SIRT1 for Metabolic Adaptation to Fasting and Exercise in Skeletal Muscle. *Cell Metab.* 11, 213–219. doi:10.1016/j.cmet.2010.02.006
- Catoire, M., Alex, S., Paraskevopoulos, N., Mattijssen, F., Evers-van Gogh, I., Schaart, G., et al. (2014). Fatty Acid-Inducible ANGPTL4 Governs Lipid Metabolic Response to Exercise. *Proc. Natl. Acad. Sci.* 111, E1043–E1052. doi:10.1073/pnas.1400889111
- Cawthorn, W. P., and Sethi, J. K. (2008). TNF- α and Adipocyte Biology. *FEBS Lett.* 582, 117–131. doi:10.1016/j.febslet.2007.11.051
- Chen, Y., Wang, Y., Zeng, K., Lei, Y.-f., Chen, X.-h., Ying, S.-c., et al. (2018). Knockdown Expression of IL-10Ra Gene Inhibits PRRSV Replication and Elevates Immune Responses in PBMCs of Tibetan Pig *In Vitro*. *Vet. Res. Commun.* 42, 11–18. doi:10.1007/s11259-017-9703-z
- Choe, S. S., Huh, J. Y., Hwang, I. J., Kim, J. I., and Kim, J. B. (2016). Adipose Tissue Remodeling: Its Role in Energy Metabolism and Metabolic Disorders. *Front. Endocrinol.* 7, 30. doi:10.3389/fendo.2016.00030
- Davies, B. S. J., Beigneux, A. P., Barnes, R. H., Tu, Y., Gin, P., Weinstein, M. M., et al. (2010). GPIHBP1 Is Responsible for the Entry of Lipoprotein Lipase into Capillaries. *Cell Metab.* 12, 42–52. doi:10.1016/j.cmet.2010.04.016
- Desaulniers, A. T., Cederberg, R. A., Mills, G. A., Lents, C. A., and White, B. R. (2017). Production of a Gonadotropin-Releasing Hormone 2 Receptor Knockdown (GNRH2 KD) Swine Line. *Transgenic Res.* 26, 567–575. doi:10.1007/s11248-017-0023-4

FUNDING

This work was supported by the National Key Research and Development Project (Grant Number 2019YFE0106800), the National Key R&D Program of China (Grant Number 2018YFD0501050), the Beijing Innovation Consortium of Agriculture Research System (Grant Number BAIC02-2018), and the Program of New Breed Development *via* Transgenic Technology (Grant Number 2016ZX080011-006).

ACKNOWLEDGMENTS

We acknowledge our colleagues in the molecular quantitative genetics team at China Agricultural University for their helpful comments on the manuscript.

SUPPLEMENTARY MATERIAL

The Supplementary Material for this article can be found online at: <https://www.frontiersin.org/articles/10.3389/fgene.2021.753725/full#supplementary-material>

- Dijk, W., Heine, M., Vergnes, L., Boon, M. R., Schaart, G., Hesselink, M. K., et al. (2015). ANGPTL4 Mediates Shuttling of Lipid Fuel to Brown Adipose Tissue during Sustained Cold Exposure. *Elife* 4, 1–13. doi:10.7554/eLife.08428
- Dijk, W., Ruppert, P. M. M., Oost, L. J., and Kersten, S. (2018). Angiopoietin-like 4 Promotes the Intracellular Cleavage of Lipoprotein Lipase by PCSK3/furin in Adipocytes. *J. Biol. Chem.* 293, 14134–14145. doi:10.1074/jbc.RA118.002426
- Fuller, T. F., Ghazalpour, A., Aten, J. E., Drake, T. A., Lusis, A. J., and Horvath, S. (2007). Weighted Gene Coexpression Network Analysis Strategies Applied to Mouse Weight. *Mamm. Genome* 18, 463–472. doi:10.1007/s00335-007-9043-3
- Glaser, C., Heinrich, J., and Koletzko, B. (2010). Role of FADS1 and FADS2 Polymorphisms in Polyunsaturated Fatty Acid Metabolism. *Metabolism* 59, 993–999. doi:10.1016/j.metabol.2009.10.022
- Greenberg, A. S., Egan, J. J., Wek, S. A., Garty, N. B., Blanchette-Mackie, E. J., and Londos, C. (1991). Perilipin, a Major Hormonally Regulated Adipocyte-specific Phosphoprotein Associated with the Periphery of Lipid Storage Droplets. *J. Biol. Chem.* 266, 11341–11346. doi:10.1016/s0021-9258(18)99168-4
- Gregoire, F. M., Smas, C. M., and Sul, H. S. (1998). Understanding Adipocyte Differentiation. *Physiol. Rev.* 78, 783–809. doi:10.1074/jbc.272.8.5128
- Haemmerle, G., Zimmermann, R., Hayn, M., Theussl, C., Waeg, G., Wagner, E., et al. (2002). Hormone-sensitive Lipase Deficiency in Mice Causes Diglyceride Accumulation in Adipose Tissue, Muscle, and Testis. *J. Biol. Chem.* 277, 4806–4815. doi:10.1074/jbc.M110355200
- Haider, S., Ballester, B., Smedley, D., Zhang, J., Rice, P., and Kasprzyk, A. (2009). BioMart Central Portal-unified Access to Biological Data. *Nucleic Acids Res.* 37, W23–W27. doi:10.1093/nar/gkp265
- Horvath, S., Zhang, B., Carlson, M., Lu, K. V., Zhu, S., Felciano, R. M., et al. (2006). Analysis of Oncogenic Signaling Networks in Glioblastoma Identifies ASPM as a Molecular Target. *Proc. Natl. Acad. Sci.* 103, 17402–17407. doi:10.1073/pnas.0608396103
- Howard, J. T., Ashwell, M. S., Baynes, R. E., Brooks, J. D., Yeatts, J. L., and Maltecca, C. (2017). Gene Co-expression Network Analysis Identifies Porcine Genes Associated with Variation in Metabolizing Fenbendazole and Flunixin Meglumine in the Liver. *Sci. Rep.* 7, 1357. doi:10.1038/s41598-017-01526-5
- Hu, Y., Tan, L.-J., Chen, X.-D., Liu, Z., Min, S.-S., Zeng, Q., et al. (2018). Identification of Novel Potentially Pleiotropic Variants Associated with Osteoporosis and Obesity Using the cFDR Method. *J. Clin. Endocrinol. Metab.* 103, 125–138. doi:10.1210/je.2017-01531

- Iwata, J., Suzuki, A., Pelikan, R. C., Ho, T.-V., Sanchez-Lara, P. A., and Chai, Y. (2014). Modulation of Lipid Metabolic Defects Rescues Cleft Palate in Tgfb β 2 Mutant Mice. *Hum. Mol. Genet.* 23, 182–193. doi:10.1093/hmg/ddt410
- Izawa, T., Rohatgi, N., Fukunaga, T., Wang, Q.-T., Silva, M. J., Gardner, M. J., et al. (2015). ASXL2 Regulates Glucose, Lipid, and Skeletal Homeostasis. *Cell Rep.* 11, 1625–1637. doi:10.1016/j.celrep.2015.05.019
- Kadioglu, O., Saeed, M. E. M., Mahmoud, N., Azawi, S., Mrasek, K., Liehr, T., et al. (2021). Identification of Novel Drug Resistance Mechanisms by Genomic and Transcriptomic Profiling of Glioblastoma Cells with Mutation-Activated EGFR. *Life Sci.* 284, 119601. doi:10.1016/j.lfs.2021.119601
- Kahn, B. B., and Flier, J. S. (2000). Obesity and Insulin Resistance. *J. Clin. Invest.* 106, 473–481. doi:10.1172/JCI10842
- Karin, M., Liu, Z.-g., and Zandi, E. (1997). AP-1 Function and Regulation. *Curr. Opin. Cell Biol.* 9, 240–246. doi:10.1016/S0955-0674(97)80068-3
- Kershaw, E. E., and Flier, J. S. (2004). Adipose Tissue as an Endocrine Organ. *J. Clin. Endocrinol. Metab.* 89, 2548–2556. doi:10.1210/jc.2004-0395
- Kogelman, L. J. A., Cirera, S., Zhernakova, D. V., Fredholm, M., Franke, L., and Kadarmideen, H. N. (2014). Identification of Co-expression Gene Networks, Regulatory Genes and Pathways for Obesity Based on Adipose Tissue RNA Sequencing in a Porcine Model. *BMC Med. Genomics* 7, 57. doi:10.1186/1755-8794-7-57
- Kogelman, L. J. A., Fu, J., Franke, L., Greve, J. W., Hofker, M., Rensen, S. S., et al. (2016). Inter-Tissue Gene Co-expression Networks between Metabolically Healthy and Unhealthy Obese Individuals. *PLoS One* 11, e0167519. doi:10.1371/journal.pone.0167519
- Koliwad, S. K., Kuo, T., Shipp, L. E., Gray, N. E., Backhed, F., So, A. Y.-L., et al. (2009). Angiopoietin-like 4 (ANGPTL4, Fasting-Induced Adipose Factor) Is a Direct Glucocorticoid Receptor Target and Participates in Glucocorticoid-Regulated Triglyceride Metabolism. *J. Biol. Chem.* 284, 25593–25601. doi:10.1074/jbc.M109.025452
- Kovrov, O., Kristensen, K. K., Larsson, E., Ploug, M., and Olivecrona, G. (2019). On the Mechanism of Angiopoietin-like Protein 8 for Control of Lipoprotein Lipase Activity. *J. Lipid Res.* 60, 783–793. doi:10.1194/jlr.M088807
- Kroupa, O., Vorrsjö, E., Stienstra, R., Mattijssen, F., Nilsson, S. K., Sukonina, V., et al. (2012). Linking Nutritional Regulation of Angptl4, Gpihbp1, and Lmfl to Lipoprotein Lipase Activity in Rodent Adipose Tissue. *BMC Physiol.* 12, 13. doi:10.1186/1472-6793-12-13
- Lallier, T. E. (2004). Semaphorin Profiling of Periodontal Fibroblasts and Osteoblasts. *J. Dent. Res.* 83, 677–682. doi:10.1177/154405910408300904
- Lane, M. D., Tang, Q.-Q., and Jiang, M.-S. (1999). Role of the CCAAT Enhancer Binding Proteins (C/EBPs) in Adipocyte Differentiation. *Biochem. Biophysical Res. Commun.* 266, 677–683. doi:10.1006/bbrc.1999.1885
- Langfelder, P., and Horvath, S. (2008). WGCNA: An R Package for Weighted Correlation Network Analysis. *BMC Bioinformatics* 9, 559. doi:10.1186/1471-2105-9-559
- Langmead, B., and Salzberg, S. L. (2012). Fast Gapped-Read Alignment with Bowtie 2. *Nat. Methods* 9, 357–359. doi:10.1038/nmeth.1923
- Langmead, B., Trapnell, C., Pop, M., and Salzberg, S. L. (2009). Ultrafast and Memory-Efficient Alignment of Short DNA Sequences to the Human Genome. *Genome Biol.* 10, R25. doi:10.1186/gb-2009-10-3-r25
- Li, L., Pan, Z., Yang, S., Shan, W., and Yang, Y. (2018). Identification of Key Gene Pathways and Coexpression Networks of Islets in Human Type 2 Diabetes. *Dmso* 11, 553–563. doi:10.2147/DMSO.S178894
- Liu, J., Jing, L., and Tu, X. (2016). Weighted Gene Co-expression Network Analysis Identifies Specific Modules and Hub Genes Related to Coronary Artery Disease. *BMC Cardiovasc. Disord.* 16, 54. doi:10.1186/s12872-016-0217-3
- Londos, C., Brasaemle, D. L., Schultz, C. J., Segrest, J. P., and Kimmel, A. R. (1999). Perilipins, ADRP, and Other Proteins that Associate with Intracellular Neutral Lipid Droplets in Animal Cells. *Semin. Cell Developmental Biol.* 10, 51–58. doi:10.1006/scdb.1998.0275
- Long, Y. C., and Zierath, J. R. (2006). AMP-activated Protein Kinase Signaling in Metabolic Regulation. *J. Clin. Invest.* 116, 1776–1783. doi:10.1172/JCI29044
- Mattijssen, F., Alex, S., Swarts, H. J., Groen, A. K., van Schothorst, E. M., and Kersten, S. (2014). Angptl4 Serves as an Endogenous Inhibitor of Intestinal Lipid Digestion. *Mol. Metab.* 3, 135–144. doi:10.1016/j.molmet.2013.11.004
- Morrison, R. F., and Farmer, S. R. (2000). Hormonal Signaling and Transcriptional Control of Adipocyte Differentiation. *J. Nutr.* 130, 3116S–3121S. doi:10.1093/jn/130.12.3116S
- Mourot, J., and Hermier, D. (2001). Lipids in Monogastric Animal Meat. *Reprod. Nutr. Dev.* 41, 109–118. doi:10.1051/rnd:2001116
- Oft, M., Heider, K.-H., and Beug, H. (1998). TGF β Signaling Is Necessary for Carcinoma Cell Invasiveness and Metastasis. *Curr. Biol.* 8, 1243–1252. doi:10.1016/S0960-9822(07)00533-7
- Ogata, H. Y., and Oku, H. (2001). The Effects of Dietary Retinoic Acid on Body Lipid Deposition in Juvenile Red Sea Bream (*Pagrus major*); a Preliminary Study. *Aquaculture* 193, 271–279. doi:10.1016/S0044-8486(00)00496-8
- Picard, F., Kurtev, M., Chung, N., Topark-Ngarm, A., Senawong, T., Machado de Oliveira, R., et al. (2004). Sirt1 Promotes Fat Mobilization in white Adipocytes by Repressing PPAR- γ . *Nature* 429, 771–776. doi:10.1038/nature02583
- Pokluzar, K., Čandek-Potokar, M., Batorek Lukač, N., Tomažin, U., and Škrlep, M. (2020). Lipid Deposition and Metabolism in Local and Modern Pig Breeds: A Review. *Animals* 10, 424. doi:10.3390/ani10030424
- Ricote, M., Li, A. C., Willson, T. M., Kelly, C. J., and Glass, C. K. (1998). The Peroxisome Proliferator-Activated Receptor- γ Is a Negative Regulator of Macrophage Activation. *Nature* 391, 79–82. doi:10.1038/34178
- Robinson, M. D., McCarthy, D. J., and Smyth, G. K. (2009). edgeR: A Bioconductor Package for Differential Expression Analysis of Digital Gene Expression Data. *Bioinformatics* 26, 139–140. doi:10.1093/bioinformatics/btp616
- Rosen, E. D., and MacDougald, O. A. (2006). Adipocyte Differentiation from the inside Out. *Nat. Rev. Mol. Cell Biol.* 7, 885–896. doi:10.1038/nrm2066
- Ross, S. E., Hemati, N., Longo, K. A., Bennett, C. N., Lucas, P. C., Erickson, R. L., et al. (2000). Inhibition of Adipogenesis by Wnt Signaling. *Science* 289, 950–953. doi:10.1126/science.289.5481.950
- Shannon, P., Markiel, A., Ozier, O., Baliga, N. S., Wang, J. T., Ramage, D., et al. (2003). Cytoscape: A Software Environment for Integrated Models of Biomolecular Interaction Networks. *Genome Res.* 13, 2498–2504. doi:10.1101/gr.1239303
- Shaulian, E., and Karin, M. (2001). AP-1 in Cell Proliferation and Survival. *Oncogene* 20, 2390–2400. doi:10.1038/sj.onc.1204383
- Shi, Z., Derow, C. K., and Zhang, B. (2010). Co-expression Module Analysis Reveals Biological Processes, Genomic Gain, and Regulatory Mechanisms Associated with Breast Cancer Progression. *BMC Syst. Biol.* 4, 74. doi:10.1186/1752-0509-4-74
- Shubham, K., Vinay, L., and Vinod, P. K. (2017). Systems-level Organization of Non-alcoholic Fatty Liver Disease Progression Network. *Mol. Biosyst.* 13, 1898–1911. doi:10.1039/c7mb00013h
- Singh, A. K., Aryal, B., Chaube, B., Rotllan, N., Varela, L., Horvath, T. L., et al. (2018). Brown Adipose Tissue Derived ANGPTL4 Controls Glucose and Lipid Metabolism and Regulates Thermogenesis. *Mol. Metab.* 11, 59–69. doi:10.1016/j.molmet.2018.03.011
- Sodhi, S. S., Ghosh, M., Song, K. D., Sharma, N., Kim, J. H., Kim, N. E., et al. (2014). An Approach to Identify SNPs in the Gene Encoding Acetyl-CoA Acetyltransferase-2 (ACAT-2) and their Proposed Role in Metabolic Processes in Pig. *PLoS One* 9, e102432. doi:10.1371/journal.pone.0102432
- Sonnenburg, W. K., Yu, D., Lee, E.-C., Xiong, W., Gololobov, G., Key, B., et al. (2009). GPIHBP1 Stabilizes Lipoprotein Lipase and Prevents its Inhibition by Angiopoietin-like 3 and Angiopoietin-like 4. *J. Lipid Res.* 50, 2421–2429. doi:10.1194/jlr.M900145-JLR200
- Tian, L., Wen, A., Dong, S., and Yan, P. (2019). Molecular Characterization of Microtubule Affinity-Regulating Kinase4 from sus Scrofa and Promotion of Lipogenesis in Primary Porcine Placental Trophoblasts. *Int. J. Mol. Sci.* 20, 1206. doi:10.3390/ijms20051206
- Trapnell, C., Roberts, A., Goff, L., Pertea, G., Kim, D., Kelley, D. R., et al. (2012). Differential Gene and Transcript Expression Analysis of RNA-Seq Experiments with TopHat and Cufflinks. *Nat. Protoc.* 7, 562–578. doi:10.1038/nprot.2012.016
- Udyavar, A. R., Hoeksema, M. D., Clark, J. E., Zou, Y., Tang, Z., Li, Z., et al. (2013). Co-expression Network Analysis Identifies Spleen Tyrosine Kinase (SYK) as a Candidate Oncogenic Driver in a Subset of Small-Cell Lung Cancer. *BMC Syst. Biol.* 7, S1. doi:10.1186/1752-0509-7-S5-S1
- Verbeke, W., Van Oeckel, M. J., Warnants, N., Viaene, J., and Boucqué, C. V. (1999). Consumer Perception, Facts and Possibilities to Improve Acceptability of Health and Sensory Characteristics of Pork. *Meat Sci.* 53, 77–99. doi:10.1016/S0309-1740(99)00036-4
- Villena, J. A., Roy, S., Sarkadi-Nagy, E., Kim, K.-H., and Sul, H. S. (2004). Desnutrin, an Adipocyte Gene Encoding a Novel Patatin Domain-

- Containing Protein, Is Induced by Fasting and Glucocorticoids. *J. Biol. Chem.* 279, 47066–47075. doi:10.1074/jbc.M403855200
- Wang, Q. Q., Yang, B., Xia, L. L., Sun, X. X., Geng, T. Y., and Gong, D. Q. (2016). Cloning of Goose Acetyl-Coenzyme A Acyltransferase 2 and its Expression Pattern in the Development of Fatty Liver. *Chinese J. Anim. Vet. Sci.* (4), 60–77. doi:10.11843/j.issn.0366-6964.2016.04.009
- Wilhelm, S. M., Carter, C., Tang, L., Wilkie, D., McNabola, A., Rong, H., et al. (2004). BAY 43-9006 Exhibits Broad Spectrum Oral Antitumor Activity and Targets the RAF/MEK/ERK Pathway and Receptor Tyrosine Kinases Involved in Tumor Progression and Angiogenesis. *Cancer Res.* 64, 7099–7109. doi:10.1158/0008-5472.CAN-04-1443
- Xing, K., Zhu, F., Zhai, L., Liu, H., Wang, Y., Wang, Z., et al. (2015). Integration of Transcriptome and Whole Genomic Resequencing Data to Identify Key Genes Affecting Swine Fat Deposition. *PLoS One* 10, e0122396. doi:10.1371/journal.pone.0122396
- Yagy, H., Chen, G., Yokoyama, M., Hirata, K., Augustus, A., Kako, Y., et al. (2003). Lipoprotein Lipase (LpL) on the Surface of Cardiomyocytes Increases Lipid Uptake and Produces a Cardiomyopathy. *J. Clin. Invest.* 111, 419–426. doi:10.1172/JCI16751
- Ye, Q., Tian, G.-P., Cheng, H.-P., Zhang, X., Ou, X., Yu, X.-H., et al. (2018). [Retraction]MicroRNA-134 Promotes the Development of Atherosclerosis via the ANGPTL4/LPL Pathway in Apolipoprotein E Knockout Mice. *Jat* 25, 244–253. doi:10.5551/jat.40212
- Yoshida, K., Shimizugawa, T., Ono, M., and Furukawa, H. (2002). Angiotensin-like Protein 4 Is a Potent Hyperlipidemia-Inducing Factor in Mice and Inhibitor of Lipoprotein Lipase. *J. Lipid Res.* 43, 1770–1772. doi:10.1194/jlr.C200010-JLR200
- Yu, G., Wang, L.-G., Han, Y., and He, Q.-Y. (2012). clusterProfiler: an R Package for Comparing Biological Themes Among Gene Clusters. *OMICS: A J. Integr. Biol.* 16, 284–287. doi:10.1089/omi.2011.0118
- Zhang, B., and Horvath, S. (2005). A General Framework for Weighted Gene Co-expression Network Analysis. *Stat. Appl. Genet. Mol. Biol.* 4, Article17. doi:10.2202/1544-6115.1128
- Zhang, Y., Wang, Y., Wang, X., Ji, Y., Cheng, S., Wang, M., et al. (2019). Acetyl-coenzyme A Acyltransferase 2 Promote the Differentiation of Sheep Precursor Adipocytes into Adipocytes. *J. Cell. Biochem.* 120, 8021–8031. doi:10.1002/jcb.28080
- Zhao, X., Chen, S., Tan, Z., Wang, Y., Zhang, F., Yang, T., et al. (2019). Transcriptome Analysis of Landrace Pig Subcutaneous Preadipocytes during Adipogenic Differentiation. *Genes* 10, 552. doi:10.3390/genes10070552
- Zhao, X., Hu, H., Lin, H., Wang, C., Wang, Y., and Wang, J. (2020). Muscle Transcriptome Analysis Reveals Potential Candidate Genes and Pathways Affecting Intramuscular Fat Content in Pigs. *Front. Genet.* 11, 877. doi:10.3389/fgene.2020.00877
- Zhou, X., Li, D., Yin, J., Ni, J., Dong, B., Zhang, J., et al. (2007). CLA Differently Regulates Adipogenesis in Stromal Vascular Cells from Porcine Subcutaneous Adipose and Skeletal Muscle. *J. Lipid Res.* 48, 1701–1709. doi:10.1194/jlr.M600525-JLR200
- Zimmermann, R., Strauss, J. G., Haemmerle, G., Schoiswohl, G., Birner-Gruenberger, R., Riederer, M., et al. (2004). Fat Mobilization in Adipose Tissue Is Promoted by Adipose Triglyceride Lipase. *Science* 306, 1383–1386. doi:10.1126/science.1100747

Conflict of Interest: XZ and YP were employed by the company Beijing Shunxin Agriculture Co., Ltd.

The remaining authors declare that the research was conducted in the absence of any commercial or financial relationships that could be construed as a potential conflict of interest.

Publisher's Note: All claims expressed in this article are solely those of the authors and do not necessarily represent those of their affiliated organizations, or those of the publisher, the editors and the reviewers. Any product that may be evaluated in this article, or claim that may be made by its manufacturer, is not guaranteed or endorsed by the publisher.

Copyright © 2022 Zhao, Liu, Pan, Liu, Zhang, Ao, Zhang, Xing and Wang. This is an open-access article distributed under the terms of the Creative Commons Attribution License (CC BY). The use, distribution or reproduction in other forums is permitted, provided the original author(s) and the copyright owner(s) are credited and that the original publication in this journal is cited, in accordance with accepted academic practice. No use, distribution or reproduction is permitted which does not comply with these terms.